Suppression of mode competition in fiber lasers by using a saturable absorber and a fiber ring

Jing Yang (杨 敬), Ronghui Qu (瞿荣辉), Guoyong Sun (孙国勇), Jianxin Geng (耿建新), Haiwen Cai (蔡海文), and Zujie Fang (方祖捷)

Shanghai Institute of Optics and Fine Mechanics, Chinese Academy of Sciences, Shanghai 201800

Received December 1, 2005

An erbium-doped fiber (EDF) laser was configured with a fiber grating, a fiber ring resonator, and a saturable absorber by using un-pumped EDF as mode selection element. The laser showed single mode operation with a narrow linewidth of 5 kHz. The mode selection mechanisms of the un-pumped EDF and the ring resonator are theoretically and experimentally analyzed.

OCIS codes: 140.0140, 140.3510, 140.4780.

Single-longitudinal-mode (SLM) fiber lasers are attractive for many applications such as wavelength-division multiplexing (WDM), coherent measurement and detection, and fiber sensors. The tunability of the single mode laser is also a hot research subject with practical importance. Fiber ring lasers usually oscillate in multi modes because they have long cavity from several to tens meters; the free spectral range (FSR) lies typically in the megahertz range, which is several orders of magnitude lower than the bandwidth of the optical filters usually used. The key to single mode operation is to suppress or even eliminate competitions between modes. It has been shown that the unidirectional ring configuration is an effective method to eliminate spatial hole burning occurring in fiber lasers and to benefit the SLM operation. An extremely short cavity with highly Er/Yb-doped fiber was reported to solve this problem[1], but its tuning range is limited (< 5 nm). The saturable absorber was used to obtain SLM operation[2], and the 40-nm tuning range was achieved[3]. A piece of un-pumped erbium-doped fiber (EDF) was used to provide mode selectivity in an erbium-doped fiber laser (EDFL), and spatial-hole burning occurring in the fiber was considered as the main mechanism[4]. A tunable band-pass filter was inserted in the fiber ring laser and 33-nm tuning range was achieved[5].

In this paper, a single mode fiber laser is described, which has a composite configuration including a fiber Bragg grating (FBG), a passive fiber ring resonator, and an un-doped EDF. The laser operating in a single mode with narrow linewidth of 5 kHz was measured. The mechanisms of the saturable absorber and the ring resonator are analyzed theoretically and experimentally.

To ensure a fiber laser operating under SLM, some different technologies are usually taken in the configuration, such as filters and saturable absorbers. Figure 1 shows the fiber laser used in the experiment. Three measures were incorporated in the setup: a FBG was connected by a 10:90 coupler to fix the central wavelength, and limit the gain spectrum in sub-nanometer range; an un-pumped EDF fused in a Sagnac loop was used as a saturable absorber; and a fiber ring resonator composed by a 10:90 coupler was used to further increase the side mode suppression; they were all connected with the ring laser through a four-port circulator.

Lengths of the laser ring, the ring resonator, and the Sagnac loop could be measured roughly by a ruler and precisely by their frequency spectra obtained by a spectrum analyzer. The measurement results were as follows. The length of laser ring with pumped EDF was 48 m corresponding to a mode spacing of 4.2 MHz. The length of the fiber ring resonator was 5 m with mode spacing of 40 MHz. Vernier effect between the two sets of modes would occur to suppress side modes in great degree. The un-pumped EDF in the Sagnac loop with length of 1.85 m played a role of saturable absorber of reducing the linewidth of the SLM.

The output was measured by a radio frequency (RF) spectrum analyzer. Figure 2 shows the measured spectra in full scale of 1 GHz, where Fig. 2(a) is the result with FBG and ring resonator, but without Sagnac loop, and Fig. 2(b) is for the case with three methods. Figure 3 shows the measured homodyne curve, which gives a typical linewidth of 5 kHz by using the commonly used method[6].

To understand the mechanism of the un-pumped EDF, its saturable characteristics were measured by using a tunable laser, a precision variable attenuator, and a power meter. Figure 4 shows the measured absorption varying with the input power at the wavelength range around 1550. It is shown that the saturation is obvious even at low power level of less than tens milliwatts.

The action of FBG in the experiment is clear as a narrow band filter. For the saturable absorption and ring resonator used in the experiment, it may be needed to analyze their detailed mechanisms and to get a physical picture of mode selections.

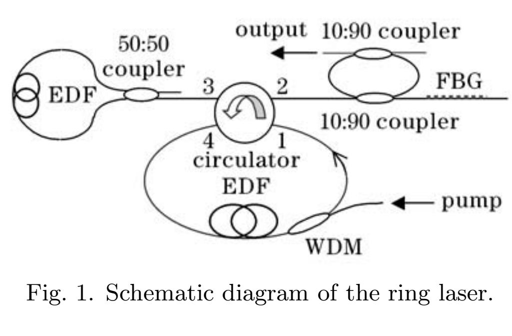

Fig. 1. Schematic diagram of the ring laser.

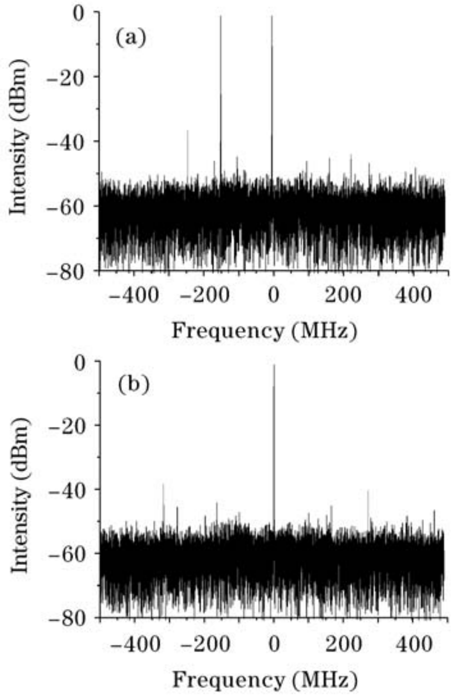

Fig. 2. RF spectra of the laser output without (a) and with (b) a saturable absorber.

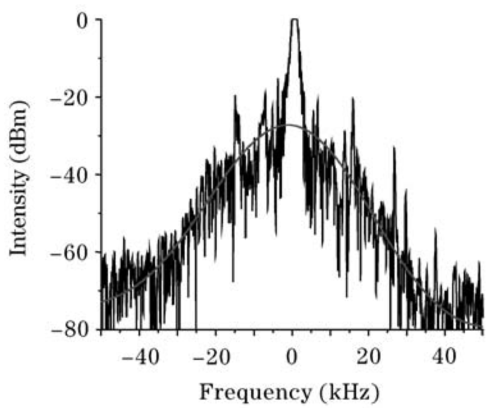

Fig. 3. Measured homodyne trace.

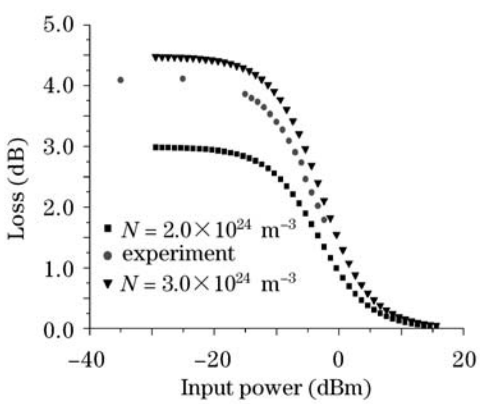

Fig. 4. Absorption as a function of input power.

A two-level model is usually used to describe an EDF. For an un-pumped EDF, optical intensity variation is governed by the Bill law, and the absorption coefficient can be written as

$$\alpha = \eta[\sigma_{12}N_1(z) - \sigma_{21}N_2(z)], \tag{1}$$

where η stands for the overlapping of optical field with the erbium distribution, σ_{21} and σ_{12} are the cross sections of transitions from the excited state with population of N_2 to ground state with N_1, and the reverse, respectively. The density of the doped erbium ions is $N_0 = N_1(z) + N_2(z)$. Under a stationary state, population of the excited state should satisfy the rate equation

$$\frac{N_2(z)}{\tau} = \frac{\eta}{h\nu A_{\text{eff}}}[\sigma_{12}N_1(z) - \sigma_{21}N_2(z)]S(z), \tag{2}$$

where S is the optical power, τ is the spontaneous emission lifetime of the excited erbium ions, and A_{eff} is the effective area of fiber.

From Eqs. (1) and (2), the absorption coefficient can be rewritten as

$$\alpha = \frac{\eta\sigma_{12}N_0}{1 + \eta\tau(\sigma_{12} + \sigma_{21})S(z)/(h\nu A_{\text{eff}})} = \frac{\alpha_0}{1 + S(z)/S_B}, \tag{3}$$

where $S_B = h\nu A_{\text{eff}}/\eta\tau(\sigma_{12} + \sigma_{21})$ is the saturation parameter. Considering the absorption coefficient as a function of power, relation between the input power $S(0)$ and output power $S(L)$ can be deduced as

$$S(L) - S(0) + S_B\{\ln[S(L)/S(0)] + \alpha_0 L\} = 0. \tag{4}$$

Equation (4) was numerically solved with parameters used in Ref. [7]: $\tau = 11.4$ ms, $\sigma_{21} = 2.7 \times 10^{-25}$ m^2, $\sigma_{12} = 3.1 \times 10^{-25}$ m^2, at the wavelength of 1550 nm; $A_{\text{eff}} = 1.26 \times 10^{-11}$ m^2 ($a = 2.0$ μm), $\eta = 0.6$, and the EDF length of 1.85 m. The calculated curves for absorption versus input power are shown in Fig. 4 with the doping densities of $N_0 = 3.0 \times 10^{24}$ and 2.0×10^{24} m^{-3} respectively. The doping level of the EDF used in the experiment is about 2.7×10^{24} m^{-3}.

The saturable absorber used in the experiment composed of an un-pumped EDF inserted in a Sagnac ring has an advantage that two inputs from opposite ports can be set with equal intensity as a 3-dB coupler is used, and therefore the standing wave established in the fiber will have a higher visibility. To estimate its effect of mode selection, an averaged absorption for a particular mode defined as $\bar{\alpha}_m = \int_0^l \alpha S_m \mathrm{d}z / \int_0^l S_m \mathrm{d}z$ was calculated by numerical simulation. The optical power can be described by a raised-cosine function of $S_m = S_{m0}(1 + \cos\beta_m z)/2$ in case of an ideal visibility is realized, where S_m and β_m are the adjusted constant and propagation constant, respectively. Then the averaged absorption can be written as

$$\bar{\alpha}_m = \int_0^l \frac{\alpha_0 S_{m0}(1 + \cos\beta_m z)\mathrm{d}z}{2 + S_B^{-1}\sum_i S_{i0}(1 + \cos\beta_i z)}$$

$$\times[\int_0^l S_{m0}(1 + \cos\beta_m z)\mathrm{d}z]^{-1}$$

$$= \frac{\alpha_0}{l}\int_0^l \frac{(1 + \cos\beta_m z)\mathrm{d}z}{2 + S_B^{-1}\sum_i S_{i0}(1 + \cos\beta_i z)}, \tag{5}$$

where β_i is the propagation constant written as $\beta_i = 2\pi n/\lambda_i$ for every longitudinal mode. For a standing wave formed in the fiber, $\lambda_i = i(2L/M)$, where M is a big integer. In simulation, the parameters were used as: EDF length $l = 1.85$ m, loop length $L \approx 4$ m, and input power of main mode $S_{m0} = 5$ mW. Equation (5) shows that the standing wave caused by saturable absorption depends on mode intensities, and there is a positive feedback when lasing. For the side modes, the loss is larger than the main lasing mode, because their interference pattern mismatches the standing wave[8].

The result of numerical calculation is shown in Fig. 5, which presents the absorption as function of mode. It is shown that the saturable absorption acts as a narrow band filter, which has a similar form as an ordinary FBG, but much narrower than FBG. It is reasonable because the grating generated in the saturable absorption fiber is much longer than ordinary FBG with length of several centimeters. Correspondingly, its linewidth is typically in the range of megahertz, much narrower than tens gigahertz of the FBG. The amplitude of the loss spectrum and their differences between the modes in Fig. 5 seem a bit smaller, but in practice the lasing will provide positive feedback to enhance the mode selection much more.

Ring resonators have attracted wide attention for applications as a narrow band filter, or a notch filter, or an optical add/drop multiplexer (OADM), and so on. Most researches are concentrated on planar waveguide devices. This work used a fiber ring resonator to connect the FBG reflector as shown in Fig. 1. The composed feedback can be described by a propagation function as

$$R = R_{\mathrm{FBG}} T_{\mathrm{ring}} = R_{\mathrm{FBG}} \frac{\kappa_1 + \kappa_2 - 2\sqrt{\kappa_1 \kappa_2} \cos \beta l_{\mathrm{r}}}{1 + \kappa_1 \kappa_2 - 2\sqrt{\kappa_1 \kappa_2} \cos \beta l_{\mathrm{r}}}, \quad (6)$$

where $(1-\kappa_1) : \kappa_1$ and $(1-\kappa_2) : \kappa_2$ are the coupling ratios of the two couplers, as shown in Fig. 1, l_{r} is the length of fiber ring. The free spectral range of a ring is

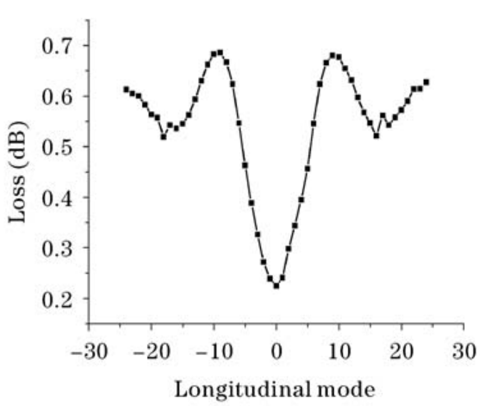

Fig. 5. Loss of a saturable absorber filter.

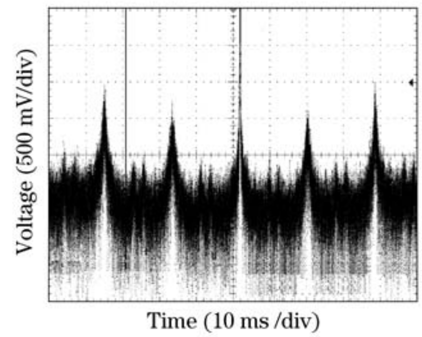

Fig. 6. RF spectrum of the fiber ring resonator.

$(\mathrm{FSR})_{\mathrm{ring}} = c/(nl_{\mathrm{r}})$, and the linewidth of each resonator mode is roughly $\delta f = \pi^{-1}(\mathrm{FSR})\sin^{-1}[(1-\kappa)/(1+\kappa)] \approx [(1-\kappa)/2\pi](\mathrm{FSR})$, where the two coupling ratios are taken as the same, and the last approximation is valid in case of $\kappa \approx 1$. Figure 6 is the frequency spectrum of a ring resonator with fiber length of 5 m and coupling ratio of 90:10, measured by an analyzer and displayed in oscilloscope with a ratio of 1 MHz/ms. It could be estimated that its FSR was about 39 MHz, and the linewidth was less than 4 MHz, which was much less than that of FBG, and in the same order of magnitude with the FSR of the ring laser.

An EDFL was investigated experimentally. By using a FBG reflection filter, a fiber ring resonator, and an un-pumped EDF saturable absorber inserted in a Sagnac loop the laser was operated in a good SLM with linewidth of 5 kHz. Theoretical analyses and simulations were presented to explain the roles of un-pumped EDF and ring resonator. This work may be helpful for further improving characteristics of SLM lasers and their applications.

R. Qu is the author to whom the correspondence should be addressed, his e-mail address is rhqu@siom.ac.cn.

References

1. K. Hsu, C. M. Miller, J. T. Kringlebotn, E. M. Taylor, J. Townsend, and D. N. Payne, Opt. Lett. **19,** 886 (1994).
2. Y. Cheng, J. T. Kringlebotn, W. H. Loh, R. I. Laming, and D. N. Payne, Opt. Lett. **20,** 875 (1995).
3. Y. W. Song, S. A. Havstad, D. Starodubov, Y. Xie, A. E. Willner, and J. Feinberg, IEEE Photon. Technol. Lett. **13,** 1167 (2001).
4. N. Kishi and T. Yazaki, IEEE Photon. Technol. Lett. **11,** 182 (1999).
5. Q. Yang, B. Yu, and S. Zhen, Journal of Anhui University (Natural Science Edition) (in Chinese) **27,** 49 (2003).
6. B. Yu, J. Qian, Y. Yang, and J. Luo, Chin. J. Lasers (in Chinese) **28,** 351 (2001).
7. G. Du and G. Chen, Science in China **28,** 535 (1998).
8. M. Horowitz, R. Daisy, B. Fischer, and J. Zyskind, Electron. Lett. **30,** 648 (1994).